

# Universal Extra-Dimensional models with boundary localized kinetic terms: Probing at the LHC

Anindya Datta<sup>1\*</sup>, Ujjal Kumar Dey<sup>1,2†</sup>, Avirup Shaw<sup>1‡</sup>, Amitava Raychaudhuri<sup>1§</sup>

<sup>1)</sup> *Department of Physics, University of Calcutta, 92 Acharya Prafulla Chandra Road, Kolkata 700009, India*

<sup>2)</sup> *Harish-Chandra Research Institute, Chhatnag Road, Jhunsi, Allahabad 211019, India*

## Abstract

In universal extra-dimensional models a conserved  $Z_2$  parity ensures the stability of the lightest Kaluza-Klein particle, a potential dark-matter candidate. Boundary-localized kinetic terms, in general, do not preserve this symmetry. We examine, in the presence of such terms, the single production of Kaluza-Klein excitations of the neutral electroweak gauge bosons and their decay to zero-mode fermion-antifermion pairs. We explore how experiments at the Large Hadron Collider at CERN can constrain the boundary-localized kinetic terms for different choices of the compactification radius.

PACS Nos: 11.10.Kk, 14.80.Rt, 13.85.-t

Key Words: Universal Extra Dimension, Kaluza-Klein, LHC

## I Introduction

The Large Hadron Collider (LHC) at CERN has opened a new vista for exploring particle physics models. Along with the search for the Higgs boson or the origin of electroweak symmetry breaking, there is also a keen interest to know about what physics lies beyond the Standard Model. That there has to be some novelty around the corner is beyond doubt, important indications being the issue of naturalness of a relatively light Higgs, the observed non-zero masses of neutrinos, and the lack of a suitable candidate for dark matter. What is unknown is the scale at which this new physics will manifest and the nature of its signal. There are many models which are being carefully examined: supersymmetry, extra dimensions, little higgs models, and the like. It is widely expected that the LHC will soon either find supporting evidence for one or the other of these models or tightly constrain them. In this work we consider a class of extra-dimensional models where all particles are exposed to an extra dimension [1]. The models under consideration here can be termed as non-minimal universal extra-dimensions (nmUED) for reasons which we elaborate in the following. We show here that LHC experiments at 8 TeV may exclude significant portions of the parameter space of this class of models.

---

\*email: adphys@caluniv.ac.in

†email: ujjaldehy@hri.res.in

‡email: avirup.cu@gmail.com

§email: palitprof@gmail.com

We explore models with one extra spacelike dimension,  $y$ , which is flat and compactified. This coordinate can thus be considered to run from 0 to  $2\pi R$ , where  $R$  is the radius of compactification. All particles – scalars, spin-1/2 fermions, and gauge bosons – are represented by five-dimensional fields which can be expressed in terms of towers of four-dimensional Kaluza-Klein (KK) states. The KK states at the  $n$ -th level for all particles have the same mass of  $n/R$ . Further, in order to incorporate chiral fermions a  $Z_2$  symmetry ( $y \leftrightarrow -y$ ) is imposed. Thus the extra dimension is compactified on an orbifold  $S^1/Z_2$ . A translation in  $y$  direction by an amount  $\pi R$  remains a symmetry of this orbifold. This symmetry leads to a conserved KK-parity given by  $(-1)^n$  where  $n$  is the KK-level. The standard model (SM) particles correspond to  $n = 0$  and are of even parity while the KK-states of the first level are odd. The conservation of KK-parity ensures that the lightest  $n = 1$  particle is absolutely stable and hence a potential dark matter candidate, the Lightest Kaluza-Klein Particle (LKP). This constitutes what is termed the Universal Extra Dimension (UED) Model.

The  $S^1/Z_2$  compactification leads to two fixed points at  $y = 0$  and  $y = \pi R$ . At these boundary points one can admit additional interaction terms between the KK-states. In fact, such terms are also necessitated as counterterms to compensate for loop-induced effects [2] of the 5-dimensional theory. In the minimal Universal Extra-Dimensional Models (mUED) [3, 4] these terms are chosen so that the 5-dimensional loop contributions are exactly compensated at the cutoff scale of the theory  $\Lambda$  and the boundary values of the corrections, e.g., logarithmic corrections to masses of KK particles, can be taken to be vanishing at the scale  $\Lambda$ . Such contributions can remove the mass degeneracy among states at the same KK-level  $n$ .

In this work we allow the boundary terms to be unrestricted by the special choice in mUED. In this sense the model can be termed non-minimal UED (nmUED). In mUED the boundary terms are equal at both fixed points – a property which may be extended to nmUED. This will preserve a discrete  $Z_2$  symmetry which exchanges  $y \longleftrightarrow (y - \pi R)$ . Here we make a further departure by allowing the boundary terms to be of different strengths at the two fixed points or even choosing the boundary term to be non-zero only at one fixed point. This leads to breaking of this  $Z_2$  symmetry and has far-reaching consequences<sup>1</sup>. For example, the  $n = 1$  excitation of the neutral gauge bosons,  $B^1$  and  $W_3^1$ , can be produced singly at the LHC and can decay to a zero-mode fermion-antifermion pair. We examine the impact of different choices of the boundary terms on the above production and decay rates and explore the prospects of detecting a signal of KK-particles through this process at the LHC.

We remark here that there is an alternate way of considering these theories as defined on a fixed interval in the extra dimension with boundary conditions applied on the fields [5]. The orbifolding alluded to above is disposed off in this formulation and the boundary conditions offer more flexibility. Our analysis below can be considered to belong to either of these formulations.

There have been several explorations of the UED Model and its variants with a view to constraining the compactification radius  $R$  and the cut-off  $\Lambda$ . To start with, an important feature of these models is that to one-loop order electroweak observables have been shown to receive

---

<sup>1</sup>This is similar to R-Parity violating interactions in supersymmetry.

finite corrections<sup>2</sup> [6]. It is therefore meaningful to compare the predictions of the theory with experimental data and obtain bounds on  $R$  and  $\Lambda$ . For example, using the muon ( $g - 2$ ) [7], flavour changing neutral currents [8, 9, 10],  $Z \rightarrow b\bar{b}$  decay [11], the  $\rho$  parameter [1, 12], and other electroweak precision tests [13, 14], it is found that  $R^{-1} \gtrsim 300 - 600$  GeV. A relatively low allowed value of  $R^{-1}$  encourages the continuing search for signatures of the model at the Tevatron and the LHC [15] and also in future facilities such as the ILC or CLIC [16].

In the next section we set up our notations by briefly reviewing the Universal Extra Dimension model and display the mode expansions of different fields. This is followed by a discussion of the nmUED scenario. Here, among other things, we present a new formulation for the fermion fields and point out how KK-number is violated by boundary-localized kinetic terms. In the next section we calculate the  $Z_2$ -parity violating coupling involving the first excitation of the neutral electroweak gauge bosons and a zero-mode fermion-antifermion pair. This coupling can lead to both the single production of this particle at the LHC and its decay resulting in a characteristic signal, relatively background free if the decay product fermion is a lepton, which is examined next. Ranges of the boundary-localized couplings which may be probed by  $20 fb^{-1}$  data from the present 8 TeV LHC run are discussed. We end with our conclusions.

## II Universal Extra Dimension

We will be considering a Universal Extra Dimension theory with one extra dimension. As a typical example, the five-dimensional Lagrangian for the SM leptons is:

$$S_{leptons} = \int d^4x dy \{ \bar{\mathcal{L}}_i(x, y)(i\Gamma^M D_M)\mathcal{L}_i(x, y) + \bar{\mathcal{E}}_i(x, y)(i\Gamma^M D_M)\mathcal{E}_i(x, y) \}, \quad (1)$$

where  $\mathcal{L}_i(\mathcal{E}_i)$  stands for a lepton doublet (singlet),  $i = 1, 2, 3$  is the generation index, and  $D_M$  the appropriate covariant derivative. Here the normal 4-dimensional spacetime is denoted by  $x(\equiv x^\mu)$  and  $y \equiv x^4$  is the compactified coordinate. Above,  $\Gamma^\mu = \gamma^\mu$  ( $\mu = 0, \dots, 3$ ) and  $\Gamma^4 = i\gamma^5$ .

In UED the 5-dimensional fields are expressed in terms of the 4-dimensional KK states. Thus in mUED the SM left- and right-chiral<sup>3</sup> lepton fields are the zero-modes in the expansions:

$$\begin{aligned} \mathcal{L}_i(x, y) &= \frac{\sqrt{2}}{\sqrt{2\pi R}} \left[ \begin{pmatrix} \nu_i \\ e_i \end{pmatrix}_L(x) + \sqrt{2} \sum_{n=1}^{\infty} \left[ \mathcal{L}_{iL}^{(n)}(x) \cos \frac{ny}{R} + \mathcal{L}_{iR}^{(n)}(x) \sin \frac{ny}{R} \right] \right], \\ \mathcal{E}_i(x, y) &= \frac{\sqrt{2}}{\sqrt{2\pi R}} \left[ e_{iR}(x) + \sqrt{2} \sum_{n=1}^{\infty} \left[ \mathcal{E}_{iR}^{(n)}(x) \cos \frac{ny}{R} + \mathcal{E}_{iL}^{(n)}(x) \sin \frac{ny}{R} \right] \right]. \end{aligned} \quad (2)$$

These fields satisfy  $\mathcal{L}_i(x, y) = -\gamma_5 \mathcal{L}_i(x, -y)$  and  $\mathcal{E}_i(x, y) = +\gamma_5 \mathcal{E}_i(x, -y)$  which ensure that the zero-modes are the SM leptons with the correct chirality. The mass of the  $n$ -th KK excitation is

<sup>2</sup>This property ceases to hold and sensitivity of various degrees to the cut-off appears at higher orders.

<sup>3</sup>The left- and right-chiral projectors are  $(1 - \gamma_5)/2$  and  $(1 + \gamma_5)/2$ , respectively.

$n/R$  irrespective of the other properties of the field. Similar expansions for the five-dimensional quark fields in terms of KK states are quite obvious.

This is the commonly used KK expansion of five-dimensional fermion fields in UED. When boundary-localized terms (BLT) come into play it is convenient to express the four component 5-dimensional fields using two component chiral spinors<sup>4</sup> as [17]:

$$\Psi_L(x, y) = \begin{pmatrix} \phi_L(x, y) \\ \chi_L(x, y) \end{pmatrix} = \sum_{n=0}^{\infty} \begin{pmatrix} \phi_n(x) f_L^n(y) \\ \chi_n(x) g_L^n(y) \end{pmatrix}, \quad (3)$$

$$\Psi_R(x, y) = \begin{pmatrix} \phi_R(x, y) \\ \chi_R(x, y) \end{pmatrix} = \sum_{n=0}^{\infty} \begin{pmatrix} \phi_n(x) f_R^n(y) \\ \chi_n(x) g_R^n(y) \end{pmatrix}. \quad (4)$$

Here we do not indicate the  $SU(2)_L$  behaviour of the fields. If, for example, the above KK expansions are for the electron, then it has to be borne in mind that  $\Psi_L(x, y)$  is one of the members of the  $SU(2)_L$  doublet  $\mathcal{L}_i(x, y)$  while  $\Psi_R(x, y)$  is the  $SU(2)_L$  singlet  $\mathcal{E}_i(x, y)$  in eq. (2). In mUED, eq. (2),  $f_i^n(y)$ ,  $g_i^n(y)$ , ( $i = L, R$ ) are either a sine or a cosine function of  $y$ . For nmUED this will no longer be the case, as we discuss later. Further, the mass of the KK-excitations will deviate from the simple  $n/R$  formula and will be solutions of a transcendental equation.

Needless to say, in UED the scalar and vector boson fields are also 5-dimensional. The lagrangian for these fields as well as their KK expansions can be similarly written down.

### III Boundary-localized terms

In nmUED one additionally considers kinetic and mass terms localized at the fixed points of the orbifold. In this work we restrict ourselves to boundary-localized kinetic terms (BLKT) only [18, 19, 20, 21, 22, 23].

We consider specifically the interaction of quarks and leptons with electroweak gauge bosons in a 5-dimensional theory with additional kinetic terms localized at the boundaries at  $y = 0$  and  $y = \pi R$ . To set the stage, we consider fermion fields  $\Psi_{L,R}$  whose zero-modes are the chiral projections of the SM fermions. To our knowledge this treatment of fermion fields with BLKT given below is new and different from all earlier ones. In terms of these fields the five-dimensional free fermion action with boundary-localized kinetic terms is written as [17]:

$$S = \int d^4x dy \left[ \bar{\Psi}_L i \Gamma^M \partial_M \Psi_L + r_f^a \delta(y) \phi_L^\dagger i \bar{\sigma}^\mu \partial_\mu \phi_L + r_f^b \delta(y - \pi R) \phi_L^\dagger i \bar{\sigma}^\mu \partial_\mu \phi_L \right. \\ \left. + \bar{\Psi}_R i \Gamma^M \partial_M \Psi_R + r_f^a \delta(y) \chi_R^\dagger i \sigma^\mu \partial_\mu \chi_R + r_f^b \delta(y - \pi R) \chi_R^\dagger i \sigma^\mu \partial_\mu \chi_R \right], \quad (5)$$

with  $\sigma^\mu \equiv (I, \vec{\sigma})$  and  $\bar{\sigma}^\mu \equiv (I, -\vec{\sigma})$ ,  $\vec{\sigma}$  being the  $(2 \times 2)$  Pauli matrices. Here  $r_f^a, r_f^b$  parametrize the strength of the boundary terms which we choose to be the same for  $\Psi_L$  and  $\Psi_R$  for illustrative purposes.

---

<sup>4</sup>The Dirac gamma matrices are in the chiral representation with  $\gamma_5 = \text{diag}(-I, I)$ .

Using eq. (3), variation of the above action leads to coupled equations for the  $y$ -dependent wave-functions of  $\Psi_L$ . These are

$$[1 + r_f^a \delta(y) + r_f^b \delta(y - \pi R)] m_n f_L^n - \partial_y g_L^n = 0, \quad m_n g_L^n + \partial_y f_L^n = 0, \quad (n = 0, 1, 2, \dots). \quad (6)$$

Analogously, using eq. (4), for the  $y$ -dependence of  $\Psi_R$  one obtains

$$[1 + r_f^a \delta(y) + r_f^b \delta(y - \pi R)] m_n g_R^n + \partial_y f_R^n = 0, \quad m_n f_R^n - \partial_y g_R^n = 0, \quad (n = 0, 1, 2, \dots). \quad (7)$$

Eliminating  $g_L^n$  and  $f_R^n$  one obtains the equations:

$$\begin{aligned} \partial_y^2 f_L^n + [1 + r_f^a \delta(y) + r_f^b \delta(y - \pi R)] m_n^2 f_L^n &= 0, \\ \partial_y^2 g_R^n + [1 + r_f^a \delta(y) + r_f^b \delta(y - \pi R)] m_n^2 g_R^n &= 0, \end{aligned} \quad (8)$$

The equations of motion above are of similar form. Below we discuss the solutions for  $f_L$  and  $g_L$ , denoted by  $f$  and  $g$  henceforth, which will also apply *mutatis mutandis* for  $f_R$  and  $g_R$ .

The boundary conditions which we impose are [19]:

$$f^n(y)|_{0^-} = f^n(y)|_{0^+}, \quad f^n(y)|_{\pi R^+} = f^n(y)|_{\pi R^-}, \quad (9)$$

$$\left. \frac{df^n}{dy} \right|_{0^+} - \left. \frac{df^n}{dy} \right|_{0^-} = -r_f^a m_n^2 f^n(y)|_0, \quad \left. \frac{df^n}{dy} \right|_{\pi R^+} - \left. \frac{df^n}{dy} \right|_{\pi R^-} = -r_f^b m_n^2 f^n(y)|_{\pi R}. \quad (10)$$

We then obtain the solutions:

$$\begin{aligned} f^n(y) &= N_n \left[ \cos(m_n y) - \frac{r_f^a m_n}{2} \sin(m_n y) \right], \quad 0 \leq y < \pi R, \\ f^n(y) &= N_n \left[ \cos(m_n y) + \frac{r_f^a m_n}{2} \sin(m_n y) \right], \quad -\pi R \leq y < 0. \end{aligned} \quad (11)$$

where the masses  $m_n$  for  $n = 0, 1, \dots$  satisfy the transcendental equation [19]:

$$(r_f^a r_f^b m_n^2 - 4) \tan(m_n \pi R) = 2(r_f^a + r_f^b) m_n. \quad (12)$$

The solutions satisfy the *orthonormality* relations:

$$\int dy [1 + r_f^a \delta(y) + r_f^b \delta(y - \pi R)] f^n(y) f^m(y) = \delta^{nm}. \quad (13)$$

The departure of eq. (11) from eq. (2) in that the wavefunctions are combinations of a sine and a cosine function rather than any one of them alone and the fact that the KK masses are solutions of eq. (12) rather than simply  $n/R$  are at the root of the novelty of nmUED over the other versions of the theory. In our discussions below for fermions we will take either symmetric boundary-localized terms, i.e.,  $r_f^a = r_f^b \equiv r_f$  or an extreme asymmetric situation where  $r_f^a \neq 0$ ,  $r_f^b = 0$ . In the latter limit eq. (12) becomes

$$\tan(m_n \pi R) = -\frac{r_f^a m_n}{2}. \quad (14)$$

Let us first pay attention to the solutions  $m_n$ . We illustrate a few issues taking as reference the above transcendental equation, eq. (14), which determines  $m_n$ . Somewhat similar considerations also apply to eq. (12). Defining  $x = m_n \pi R$  and  $y = r_f^a / 2\pi R$  the equation becomes  $\tan x = -y x$ . We require the solutions  $x$  as the *real* parameter  $y$  varies. It is worth bearing in mind that irrespective of the value of  $y$  one root is  $x = 0$  which corresponds to the zero-mode which receives no corrections from the BLKT. Besides the zero-mode, our focus for any  $y$  is on those solutions which correspond to *real*  $m_n$  and in particular in this work on the  $n = 1$  state which is the smallest root after the zero-mode. To start with, for vanishing BLKT parameters (i.e.,  $y = 0$ ), the solutions are simply  $\pm \frac{n\pi}{R}$  ( $n$  being any integer including 0), which is the case of basic UED. With non-zero BLKTs ( $y \neq 0$ ), the  $n = 1$  real root can be determined graphically for both positive and negative<sup>5</sup>  $y$ . They correspond one-to-one with the solutions in the absence of BLKT but are always smaller (larger) than  $n/R$  for the  $n$ th mode for positive (negative)  $y$ . It is noteworthy that in the mUED model, where the radiative corrections are calculated in the framework of the Standard Model gauge group, the mass of the  $n$ th mode is more than  $n/R$  (i.e., as for  $y < 0$ ) and is in a one-to-one correspondence with the mass spectra of KK-modes [3]. Here we focus on the real roots of eqs. (12) and (14) for positive as well as negative values of  $y$ .

Over and above the real roots of eq. (14), for  $0 > y > -1$  one also has complex roots in conjugate pairs<sup>6</sup>. These complex solutions for  $m_n$  are unphysical. The inclusion of a BLKT, however small, should not enhance the multiplicity of the Kaluza-Klein states – the real solutions having already matched the count.

The constant  $N_n$  can be determined from orthonormality and is

$$N_n = \sqrt{\frac{2}{\pi R}} \left[ \frac{1}{\sqrt{1 + \frac{r_f^2 m_n^2}{4} + \frac{r_f}{\pi R}}} \right], \quad (15)$$

for symmetric boundary terms.

For the asymmetric case when  $r_f^b = 0$  and we use  $r_f^a \equiv r_f$  one has

$$N_n = \sqrt{\frac{2}{\pi R}} \left[ \frac{1}{\sqrt{1 + \frac{r_f^2 m_n^2}{4} + \frac{r_f}{2\pi R}}} \right]. \quad (16)$$

In our work we will deal only with the zero-modes and the  $n = 1$  excitations of the five-dimensional fermion fields.

Now we turn to the five-dimensional gauge field,  $G_N$  ( $N = 0 \dots 4$ ), where  $G$  can be either  $W_3$

---

<sup>5</sup>For  $y < -1$ , i.e.,  $r_f^a < -2\pi R$ , the squared norm of the solution,  $|N_n|^2$ , can become negative. See, for example, eq. (16) below for  $n = 0 \Rightarrow m_n = 0$ . In the following we will consider  $y > -1$ .

<sup>6</sup>For  $n = 0$  these complex roots are pure imaginary (for  $0 > r_f^a > -2\pi R \Rightarrow 0 > y > -1$ ); a point noted earlier [20].

or  $B$ . The action with boundary kinetic terms can be similarly written as

$$S = -\frac{1}{4} \int d^4x dy [F_{MN}F^{MN} + r_G^a \delta(y) F_{\mu\nu}F^{\mu\nu} + r_G^b \delta(y - \pi R) F_{\mu\nu}F^{\mu\nu}], \quad (17)$$

where  $F_{MN} = (\partial_M G_N - \partial_N G_M)$  and  $r_G^a, r_G^b$ , the strengths of the boundary terms which are varied in our analysis<sup>7</sup>. We will also comment on an extreme asymmetric case,  $r^a \neq 0$  and  $r^b = 0$ .

The expansion of the gauge field will be:

$$G_\mu(x, y) = \sum_{n=0}^{\infty} G_\mu^{(n)}(x) a^n(y), \quad G_4(x, y) = \sum_{n=0}^{\infty} G_4^{(n)}(x) b^n(y), \quad (18)$$

where the functions  $a^n(y)$  and  $b^n(y)$  are determined by the boundary conditions as discussed below. It is convenient to make the gauge choice:  $G_4 = 0$ .

The functions  $a^n(y)$  satisfy:

$$\partial_y^2 a^n(y) + [1 + r^a \delta(y) + r^b \delta(y - \pi R)] m_n^2 a^n(y) = 0. \quad (19)$$

We use the boundary conditions

$$a^n(y)|_{0^-} = a^n(y)|_{0^+}, \quad a^n(y)|_{\pi R^+} = a^n(y)|_{\pi R^-}, \quad (20)$$

$$\left. \frac{da^n}{dy} \right|_{0^+} - \left. \frac{da^n}{dy} \right|_{0^-} = -r^a m_n^2 a^n(y)|_{0}, \quad \left. \frac{da^n}{dy} \right|_{\pi R^+} - \left. \frac{da^n}{dy} \right|_{\pi R^-} = -r^b m_n^2 a^n(y)|_{\pi R}. \quad (21)$$

which imply that the masses  $m_n$  are solutions of:

$$(r^a r^b m_n^2 - 4) \tan(m_n \pi R) = 2(r^a + r^b) m_n. \quad (22)$$

The roots of the above transcendental equation, which may be obtained numerically, are the extra-dimensional contributions,  $m_G^{(n)} \equiv m_n$ , to the masses of the KK modes<sup>8</sup> of the  $B$  and  $W$ . In our discussion below we find it convenient to use  $\Delta r = r^b - r^a$ .

Eq. (12) satisfied by KK fermions and eq. (22) valid for KK gauge bosons are of identical form. It applies to the Higgs scalars as well. We discuss the solutions together bearing in mind that for fermions and the Higgs scalars we take the BLKTs at the two fixed points to be always equal, i.e.,  $\Delta r = 0$ . In this work we are interested only in the  $n = 1$  KK modes. In fig. 1, we plot the dimensionless quantity  $M_{(1)} \equiv m^{(1)} R$ . In the left panel we show the variation of  $M_{(1)}$  with  $R^a \equiv r^a/R$  in the symmetric limit when  $\Delta r = 0$  and applies to the  $n = 1$  fermion and Higgs boson states. It also gives the extra-dimensional contribution to the gauge boson mass,  $m_G^{(1)}$ , in the special case when the BLKTs are symmetric. When  $R^a = 0$ , i.e., no BLKT

<sup>7</sup>In the remainder of this section we drop the subscript  $G$  on the brane-localized couplings for the gauge boson:  $r^a \equiv r_G^a$  and  $r^b \equiv r_G^b$ .

<sup>8</sup>As discussed below, the KK modes also receive a contribution to their masses from spontaneous breaking of the electroweak symmetry.

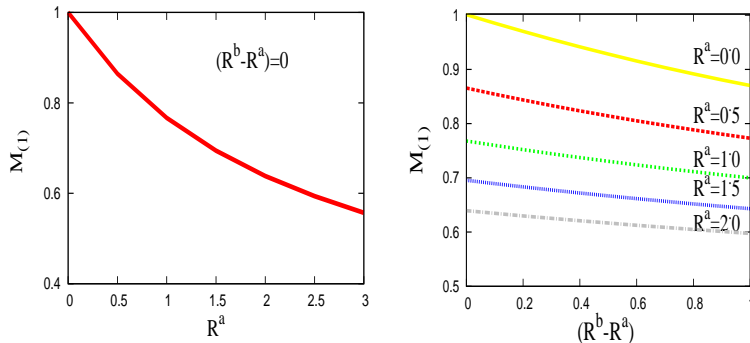


Figure 1: Variation of  $M_{(1)} \equiv m^{(1)}R$  with the BLKT strength  $R^a \equiv r^a/R$  when  $R^a = R^b$  (left) and variation of  $M_{(1)}$  with  $\frac{\Delta r}{R} \equiv (R^b - R^a)$  for different values of  $R^a$  (right). The left panel applies to fermions, gauge bosons, and Higgs scalars when the BLKTs are symmetric. Note that larger  $R^a$  yields a smaller mass in both panels. ‘a’ and ‘b’ correspond to the fixed points  $y = 0$  and  $\pi R$ , respectively.

at all, one gets  $m^{(1)} = R^{-1}$ , as expected. Keeping  $R^a = R^b$ , one finds that  $m^{(1)}$  monotonically decreases as the BLKT strength  $R^a$  increases. In the right panel,  $M_{(1)}$  is displayed as a function of the asymmetry parameter  $(R^b - R^a)$ , for several choices of  $R^a$ . When  $R^a \neq R^b$ , for a fixed  $R^a$ ,  $m^{(1)}$  falls as  $\Delta r$  grows but this reduction is not very steep for the range of  $\Delta r$  that we consider. In the right panel the range of  $(R^b - R^a)$  and the values of  $R^a$  are chosen to match with those which have been used later. Notice that the mass of the  $n = 1$  state for a particular  $R^a$  always remains more than that corresponding to any larger  $R^a$  for the entire variation of  $(R^b - R^a)$ . So, notwithstanding the value of  $(R^b - R^a)$ , the ordering of masses within the  $n = 1$  level can be determined just on the basis of the corresponding  $R^a$ s. This will be useful later in deciding which state is the LKP.

In the extreme asymmetric case that we consider ( $r^a \neq 0$ ,  $r^b = 0$ ) for the fermions, gauge bosons, and the Higgs scalars while eq. (19) continues to hold, (22) reduces to

$$\tan(m_n \pi R) = -\frac{r^a m_n}{2}. \quad (23)$$

In fig. 2, we show the variation of  $M_{(1)}$  with  $R^a$  when the BLKT is present only at  $y = 0$ . Here again  $m^{(1)}$  equals  $R^{-1}$  when  $R^a = 0$  and falls with increasing  $R^a$  asymptotically approaching the value  $0.5R^{-1}$ .

It is to be noted that the mass  $M_{(1)}$  is determined entirely by the BLKT parameters,  $R^a, R^b$  and the compactification radius  $R$ . The gauge coupling is not involved. Therefore this discussion applies for both  $W_3^1$  and  $B^1$  so long as the appropriate BLKT parameters are used.

Before proceeding further it may be worthwhile to identify the neutral electroweak gauge boson mass eigenstates. The electroweak gauge boson eigenstates in a five-dimensional theory with BLKT have been discussed in [22]. We have checked that for the range of BLKT parameters which we entertain the mixing between states of different KK level,  $n$ , is very small and may be

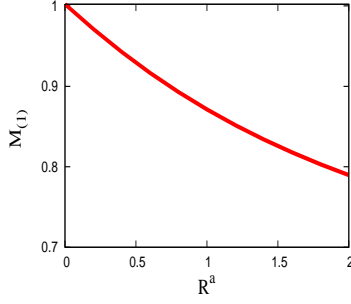


Figure 2: Variation of  $M_{(1)}$  with  $R^a$  when the BLKT is present only at the  $y = 0$  fixed point, i.e.,  $R^b = 0$ . The results are valid for fermions, gauge bosons, and Higgs scalars.

ignored. Further, only if the BLKT parameters for the  $B$  and  $W$  gauge bosons are equal or very nearly equal the mixing between  $B^1$  and  $W_3^1$  is substantial, it being equal to the zero-mode weak mixing angle in the case of equality. If  $(r_B - r_W)/R$  is as small as 0.1 this mixing is already negligible. This can be checked from the mass matrix which we now discuss.

The mass matrix for the  $n = 1$  neutral electroweak gauge bosons receives contributions from two sources: one originates from the spontaneous breaking of the electroweak symmetry and the other due to the extra-dimensional contribution discussed above. When taken together one has the mass matrix:

$$M_{W_3^1 B^1} = \begin{pmatrix} \frac{g^2 v^2}{4} \frac{S_W}{S_H} I_{W_3 W_3} + m_{W_3}^{(1)2} & -\frac{gg' v^2}{4} \frac{\sqrt{S_W S_B}}{S_H} I_{W_3 B} \\ -\frac{gg' v^2}{4} \frac{\sqrt{S_W S_B}}{S_H} I_{W_3 B} & \frac{g'^2 v^2}{4} \frac{S_B}{S_H} I_{BB} + m_B^{(1)2} \end{pmatrix}, \quad (24)$$

where

$$I_{ij} = \int_0^{\pi R} (1 + r_h \{\delta(y) + \delta(y - \pi R)\}) a_i^1(y) a_j^1(y) dy, \quad (i, j = W_3, B). \quad (25)$$

Here  $r_h$  is the strength of the BLKT for the Higgs scalar, taken to be equal<sup>9</sup> at  $y = 0$  and  $\pi R$ . As usual,  $R_h = r_h/R$ . Also,

$$a_{W_3}^1(y) = N_{W_3}^{(1)} \left[ \cos(m_{W_3}^{(1)} y) - \frac{r_W^a y}{2} \sin(m_{W_3}^{(1)} y) \right], \quad (26)$$

and

$$a_B^1(y) = N_B^{(1)} \left[ \cos(m_B^{(1)} y) - \frac{r_B^a y}{2} \sin(m_B^{(1)} y) \right], \quad (27)$$

with  $N_{W_3}^{(1)}$ ,  $N_B^{(1)}$  being the normalisation factors and  $r_G^a, r_G^b$ , ( $G \equiv W, B$ ), the strengths of the boundary terms at  $y = 0$  and  $\pi R$  respectively for the gauge bosons.

---

<sup>9</sup>When we consider the asymmetric option of BLKTs at one fixed point only, the same is the case for the Higgs scalar as well.

Further, the five-dimensional gauge couplings  $g_5, g'_5$  and the vacuum expectation value (vev)  $v_5$  are related to the usual couplings  $g, g'$  respectively and the vev  $v$  defined in four dimensions through

$$g_5 = g \sqrt{\pi R S_W}, \quad g'_5 = g' \sqrt{\pi R S_B}, \quad v_5 = v / \sqrt{\pi R S_H}, \quad (28)$$

where

$$S_W = \left(1 + \frac{R_W^a + R_W^b}{2\pi}\right), \quad S_B = \left(1 + \frac{R_B^a + R_B^b}{2\pi}\right), \quad S_H = \left(1 + \frac{R_h}{\pi}\right). \quad (29)$$

A few comments about the mass matrix in eq. (24) may not be out of place. The matrix is in the  $W_3^1 - B^1$  basis<sup>10</sup>. To estimate the different terms in the matrix notice that the  $S_i$  are  $\mathcal{O}(1)$  as are the overlap integrals  $I_{ij}$ . So the contributions to the mass matrix from the symmetry breaking are  $\mathcal{O}(v^2)$ . The order of the extra-dimensional contributions,  $m_G^{(1)2}$ , is set by  $(1/R)^2$  and is always much larger by far. As a consequence to a good approximation these terms determine the mass eigenvalues and the mixing is negligible for  $(R_W - R_B) \sim 0.1$  or larger<sup>11</sup>. So, in our discussion below we take  $B^1$  and  $W_3^1$  to be the neutral electroweak gauge eigenstates for the  $n = 1$  KK-level.

## IV Coupling of $B^1$ and $W_3^1$ with zero-mode fermions

We have now all the ingredients needed to calculate the coupling of the states  $W_3^1$  and  $B^1$  to two zero-mode fermions  $f^{(0)}$ . Here  $f^{(0)}$  could be SM quarks or leptons. We separately discuss two cases alluded to earlier. In the first, the strength of the boundary-localized couplings for fermions and Higgs scalars are of the same strength at both fixed points while for the gauge bosons we allow a variation of the strengths. In the second case, for the fermion, the Higgs scalar, as well as the gauge bosons we assume that the BLKT are present at only the  $y = 0$  fixed point.

### IV.1 Symmetric fermion BLKT, general gauge boson BLKT

Here we assume for the fermions (Higgs scalars)  $r_f^a = r_f^b = r_f$  ( $r_h^a = r_h^b = r_h$ ) while for the gauge bosons,  $B^1$  and  $W_3^1$ ,  $r^a$  and  $r^b$  can be different in general. Later, when we examine the prospects at the LHC, we take  $r_W^a \neq r_B^a$  but keep  $r_W^a - r_W^b = r_B^a - r_B^b$ . We choose  $R_h \equiv r_h/R = -1.1$ . The results are not very sensitive to the exact value of  $R_h$ . Our chosen value ensures that the  $H^1$  is always heavier than the  $B^1$  and  $W_3^1$ .

Below we discuss the case for a generic gauge boson  $G^1$ , which could be either of  $B^1$  or  $W_3^1$ .

---

<sup>10</sup>We have checked that mixing with states of  $n \neq 1$  is very small.

<sup>11</sup>If  $R_W = R_B$  then the dominant diagonal terms are equal and do not contribute to the mixing and simply shift the masses of the eigenstates. In this case the mixing between  $W_3^1$  and  $B^1$  is just as in the Standard Model with  $\tan \theta = g'/g$ .

The  $y$ -dependent wave-functions of our interest here are found to be

$$f_L^0 = g_R^0 = \frac{1}{\sqrt{\pi R(1 + R_f/\pi)}}, \quad (30)$$

and

$$a^1 = \mathcal{N}_1^a \left[ \cos\left(\frac{M_{(1)}y}{R}\right) - \frac{R^a M_{(1)}}{2} \sin\left(\frac{M_{(1)}y}{R}\right) \right], \quad (31)$$

with

$$\mathcal{N}_1^a = \sqrt{\frac{1}{\pi R}} \sqrt{\frac{8(4 + M_{(1)}^2 R^{b^2})}{2\left(\frac{R^a + R^b}{\pi}\right)(4 + M_{(1)}^2 R^a R^b) + (4 + M_{(1)}^2 R^{a^2})(4 + M_{(1)}^2 R^{b^2})}},$$

where we have used as earlier  $M_{(1)} \equiv m_G^{(1)} R$ , and the scaled dimensionless variables

$$R_f \equiv r_f/R, \quad R^a \equiv r_G^a/R, \quad \text{and} \quad R^b \equiv r_G^b/R. \quad (32)$$

Using the above we calculate

$$\begin{aligned} g_{G^1 f^0 f^0} &= g_5(G) \int_0^{\pi R} (1 + r_f \{\delta(y) + \delta(y - \pi R)\}) f_L^0 f_L^0 a^1 dy \\ &= g_5(G) \int_0^{\pi R} (1 + r_f \{\delta(y) + \delta(y - \pi R)\}) g_R^0 g_R^0 a^1 dy \\ &= \frac{g(G) \sqrt{S_G}}{\left(1 + \frac{R_f}{\pi}\right)} \mathcal{N}_1^a \left[ \frac{\sin(\pi M_{(1)})}{\pi M_{(1)}} \left\{ 1 - \frac{M_{(1)}^2 R^a R_f}{4} \right\} \right. \\ &\quad \left. + \frac{R^a}{2\pi} \{\cos(\pi M_{(1)}) - 1\} + \frac{R_f}{2\pi} \{\cos(\pi M_{(1)}) + 1\} \right]. \end{aligned} \quad (33)$$

The physics consequences of these couplings are discussed in the next section. We only wish to point out here that it can be readily seen using eq. (22) that if  $R^a = R^b$ , i.e., the BLKTs are symmetric at  $y = 0$  and  $y = \pi R$  for *both* the fermion and the gauge boson, then the coupling in eq. (33) vanishes. This can be traced to a  $[y \longleftrightarrow (y - \pi R)] Z_2$  symmetry of the theory for this choice which forbids an  $n = 1$  state to couple exclusively to zero modes.

For illustrative purposes we plot in fig. 3 the square of the coupling as a function of  $(R^b - R^a)$  for several values of  $R^a$ . The three panels correspond to representative values of  $R_f$ . In any of these panels the symmetric BLKT case is obtained when  $\Delta r = 0$ . In this limit the  $Z_2$  parity becomes operative and  $G^1$  being odd under this symmetry the coupling vanishes. The choice  $r^a = 0$  implies a set up with the gauge boson BLKT at one fixed point only while the fermion BLKTs are symmetrically distributed.

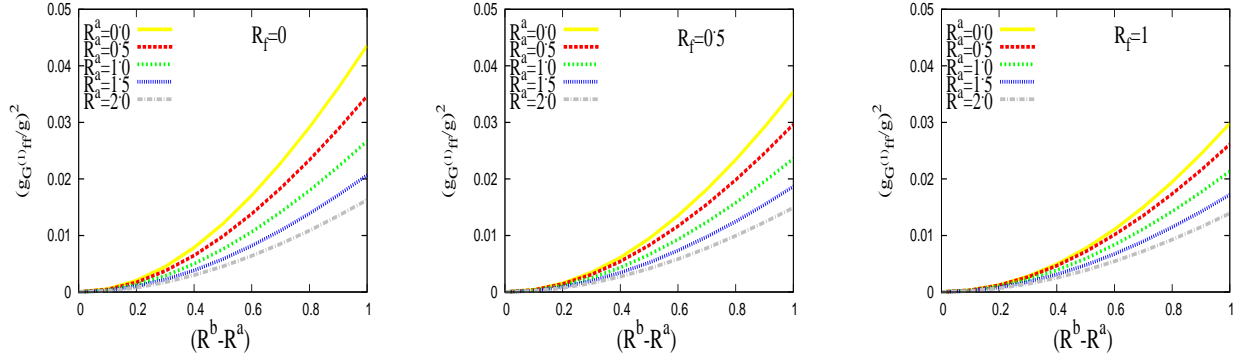


Figure 3: Variation of the square of the KK-parity violating coupling (between  $G^1 \equiv B^1$  or  $W_3^1$  and a pair of zero-mode fermions) with  $(R^b - R^a)$  for several choices of  $R^a$ . The panels correspond to different  $R_f$ .

## IV.2 Fermion and gauge boson BLKT at one fixed point only

Now we turn to the case which could be considered the most asymmetric one, namely, the boundary-localized kinetic terms for the fermion, the Higgs scalar and the gauge boson are only at the fixed point  $y = 0$  and none at  $y = \pi R$ . The  $y$ -dependent wave-functions in this case are

$$f_L^0 = g_R^0 = \frac{1}{\sqrt{\pi R(1 + R_f/2\pi)}}, \quad (34)$$

and

$$a^1 = \sqrt{\frac{1}{\pi R}} \sqrt{\frac{2}{1 + \left(\frac{R^a M_{(1)}}{2}\right)^2 + \frac{R^a}{2\pi}}} \left[ \cos\left(\frac{M_{(1)} y}{R}\right) - \frac{R^a M_{(1)}}{2} \sin\left(\frac{M_{(1)} y}{R}\right) \right], \quad (35)$$

where  $R^a \equiv r^a/R$ . With these we find in this case

$$\begin{aligned} g_{G^1 f^0 f^0} &= g_5(G) \int_0^{\pi R} [1 + r_f \delta(y)] f_L^0 f_L^0 a^1 dy \\ &= g_5(G) \int_0^{\pi R} [1 + r_f \delta(y)] g_R^0 g_R^0 a^1 dy \\ &= \frac{\sqrt{2} g(G) \sqrt{S_G}}{\left(1 + \frac{R_f}{2\pi}\right) \sqrt{1 + \left(\frac{R^a M_{(1)}}{2}\right)^2 + \frac{R^a}{2\pi}}} \left(\frac{R_f - R^a}{2\pi}\right). \end{aligned} \quad (36)$$

In fig. 4 we plot the square of the above coupling strength as a function of  $R^a$  for several choices of  $R_f$ . It is seen that the strength of the coupling is roughly of the same order as in the case discussed earlier. A noteworthy feature is that the coupling vanishes when  $R^a = R_f$ .

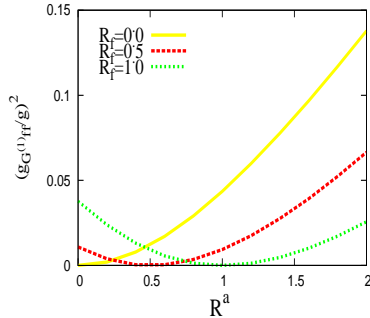


Figure 4: Variation of the square of the KK-parity violating coupling (between  $G^1 \equiv B^1$  or  $W_3^1$  and a pair of fermions) with  $R^a$  for different choices of  $R_f$  when the fermion and boson BLKTs are present only at one of the fixed points.

## V $B^1$ or $W_3^1$ production and decay

We are now in a position to discuss some phenomenological signals of nmUED. In the following we will restrict our discussion only to the prospects at the LHC. Furthermore, our focus will be on the case where KK-parity is broken as a consequence of having unequal gauge boson BLKT parameters at the orbifold fixed points. Though for  $B^1$  and  $W_3^1$  we choose different BLKT strengths we keep  $(R_G^a - R_G^b)$  to be the same for both so that the superscript  $G$  can be dispensed with in the difference. We also explore the situation where the BLKTs are present only at one of the two fixed points. Here too we consider different BLKTs for  $B^1$  and  $W_3^1$ . The necessary framework for the analyses has already been set up in the previous sections.

At the LHC we are interested to investigate the resonant production of the  $n = 1$  KK-excitations of EW gauge bosons, via the process  $pp (q\bar{q}) \rightarrow G^1$  followed by  $G^1 \rightarrow l^+l^-$  where  $G^1$  is either of  $B^1$  and  $W_3^1$  and  $l^\pm$  could be either  $e^\pm$  or  $\mu^\pm$ .

From now onwards for the SM particles we will not explicitly write the KK-number ( $n = 0$ ) as a superscript. The particles with no superscripts are implied to be the SM particles. The final state leads to two leptons ( $e$  or  $\mu$ ), with invariant mass peaked at  $m_{G^1}$ . It should be noted that both the production and the decay of  $n = 1$  KK-excitations of electroweak gauge bosons are driven by KK-parity violating couplings which vanish unless the strengths of the BLKT parameters localized at the two fixed points are different, i.e.,  $(R^b - R^a) \neq 0$ . If in future such a signature is observed at the LHC, then it would be a good channel for the determination of such KK-parity violating couplings.

An analytic expression for the production cross section in proton proton collisions can be written in a compact form :

$$\sigma(pp \rightarrow G^1 + X) = \frac{4\pi^2}{3m_{G^1}^3} \sum_i \Gamma(G^1 \rightarrow q_i \bar{q}_i) \int_\tau^1 \frac{dx}{x} \left[ f_{\frac{q_i}{p}}(x, m_{G^1}^2) f_{\frac{\bar{q}_i}{p}}(\tau/x, m_{G^1}^2) + q_i \leftrightarrow \bar{q}_i \right] \quad (37)$$

Here,  $q_i$  and  $\bar{q}_i$  stand for a generic quark and the corresponding antiquark of the  $i$ -th flavour respectively.  $\Gamma(G^1 \rightarrow q_i \bar{q}_i)$  represents the decay width of  $G^1$  into a quark and antiquark pair of the  $i$ th flavour.  $\tau \equiv m_{G^1}^2/S_{PP}$ , where  $\sqrt{S_{PP}}$  is the proton proton centre of momentum energy. The  $f$ s are quark or antiquark distribution functions within a proton.

In case of  $B^1$  production,  $\Gamma = (g_{G^1 q \bar{q}}'^2/32\pi) [(Y_L^q)^2 + (Y_R^q)^2] m_{B^1}$  (with  $Y_L^q$  and  $Y_R^q$  being the weak-hypercharges for the left- and right-chiral quarks), while for  $W_3^1$  one has  $\Gamma = (g_{G^1 q \bar{q}}^2/128\pi) m_{W_3^1}$ .  $g_{G^1 q \bar{q}}^{(\prime)}$  is the KK-parity violating coupling among SM quarks and  $W_3^1$  ( $B^1$ ) as given in eqs. (33) and (36). In the above cross section expressions  $m_{G^1}$  stands for the mass eigenvalue of the gauge boson  $n = 1$  excitation resulting from the matrix in eq. 24.

To obtain the numerical values of the cross sections, we use a parton level Monte Carlo code with parton distribution functions as parametrized in CTEQ6L [24]. We take the  $pp$  c.m. energy to be 8 TeV. Renormalisation (for  $\alpha_s$ ) and factorisation scales (in the parton distributions) are set at  $m_{G^1}$ .

To make our estimate of signal cross section more realistic, a simple toy calorimeter simulation has been implemented with the following criteria:

- $p_T^\ell > 20$  GeV.
- The calorimeter coverage (for leptons) is  $|\eta| < 3.0$ .
- A cone algorithm with  $\Delta R = \sqrt{\Delta\eta^2 + \Delta\phi^2} = 0.5$  has been used for isolation of leptons.

Once produced,  $B^1$  ( $W_3^1$ ) will decay via similar KK-parity violating couplings to SM quarks and leptons and, if kinematically allowed, to  $f^1 \bar{f}$  (or to  $f \bar{f}^1$ ) via KK-conserving couplings. We focus on the KK-parity violating leptonic decays which provide a cleaner environment at the LHC. For simplicity we assume an universal coefficient  $r_f$  for the BLKTs involving all SM fermions. If kinematically allowed (broadly when  $R_f > R_G$ ), the KK-conserving decay rates can be substantial and in such situations the branching ratios (BRs) for KK-violating decay rates are small. This behaviour is exemplified in fig. 5 where we plot the BR of the KK-number violating decay as a function of  $R_B^a$  ( $R_W^a$ ) in the left (right) panel. Note how rapidly (log scale) the BR falls when the KK-conserving decays open up ( $R_f > R_{B,W}^a$ ).

However, when the KK-conserving decays are kinematically disallowed, decays to a SM fermion anti-fermion pair are the only possible modes and hence the branching ratios become independent of the input BLKT parameters. Consequently, the decay rates of  $B^1$  to different fermions are proportional to the sum of the squares of the respective weak hypercharges  $[(Y_L^f)^2 + (Y_R^f)^2]$  of the left- and right-chiral species.  $W_3^1$ , on the other hand, decays democratically with branching ratio of  $\frac{1}{21}$  to each species of left-handed zero-mode fermions. This immediately tells us that the decay branching ratio of  $B^1$  ( $W_3^1$ ) to  $e^+e^-$  or  $\mu^+\mu^-$  is approximately  $\frac{30}{103}$  ( $\frac{2}{21}$ ), which is also evident from the plots in fig. 5.

Final states with dileptons arise in the SM mainly from resonance  $Z$ -production or Drell-Yan (DY) production. The first of these can be easily vetoed as in this case the dilepton invariant

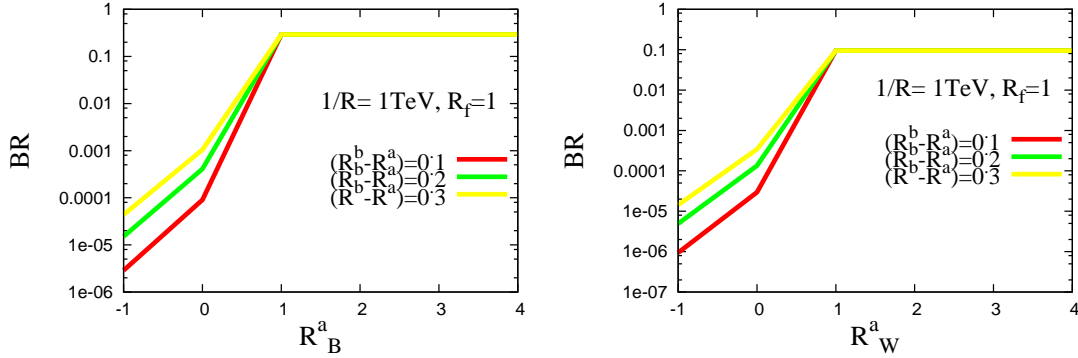


Figure 5: Branching ratios of  $B^1$  ( $W_3^1$ ) to  $e^+e^-$  or  $\mu^+\mu^-$  as a function of the BLKT parameters  $R_B^a$  ( $R_W^a$ ) are shown in the left (right panels) for several choices of  $(R^b - R^a)$ .  $R^{-1} = 1$  TeV and  $R_f = 1$  are chosen. Notice that when  $R_B^a$  ( $R_W^a$ ) falls below 1, the  $n = 1$  fermion is lighter and KK-number conserving decays reduce the BR drastically.

mass peaks around  $m_Z$ . We find that for 10 GeV bins around 700 (800) GeV the DY cross section is 2.29 (1.56)  $fb$ . This DY background though non-negligible is such that for the  $W_3^1$  and  $B^1$  masses which we consider  $S/\sqrt{B} \geq 5$  can be achieved for 20  $fb^{-1}$  integrated luminosity.

Before embarking on a detailed exploration it may be useful to set the perspective by comparing the signal cross section with the backgrounds noted above. For example, we find that with  $R^{-1} = 1$  TeV,  $R_f = 1$  and  $R_W^a = R_B^a = 1.5$  which implies  $(R_B^a - R_W^a) = 0$ , and  $(R^b - R^a) = 0.32$ , one gets  $m_{B^1}(m_{W_3^1}) \sim 675$  (676) GeV and the cross section for  $B_1(W_3^1)$  production is 52.1 (39.1) fb. When the cross sections are folded with the branching ratios one expects 303 (74) events from  $B^1$  ( $W^1$ ) production for 20  $fb^{-1}$  integrated luminosity. Of course, the  $B^1(W_3^1)$  coupling and hence the production rate depend on the input parameters and it becomes 48.5 (38.5)  $fb$  for  $R^{-1} = 1.0$  TeV,  $R_f = R_W^a = R_B^a = 1$ , and  $(R^b - R^a) = 0.32$  when  $m_{B^1}(m_{W_3^1}) \sim 742$  (743) GeV leading to 282 (73) events. Therefore we will not undertake any further effort to estimate the SM background.

We are all-equipped now to present the results. Rather than displaying the number of events as a function of the BLKT parameters, in Figs. 6 and 7 we have plotted the iso-event curves<sup>12</sup> (40 events with 20  $fb^{-1}$  luminosity for LHC running at 8 TeV).

## V.1 Symmetric fermion BLKT, general gauge boson BLKT

Fig. 6 is for the case when the fermion BLKTs are symmetric at the two fixed points while the gauge BLKTs are not. We show in this case the iso-event curves in the  $(R^b - R^a) - (R_B^a - R_W^a)$

<sup>12</sup>The requirement here is that electron *plus* muon events together resulting from  $W_3^1$  and  $B^1$  production and decay add up to 40.

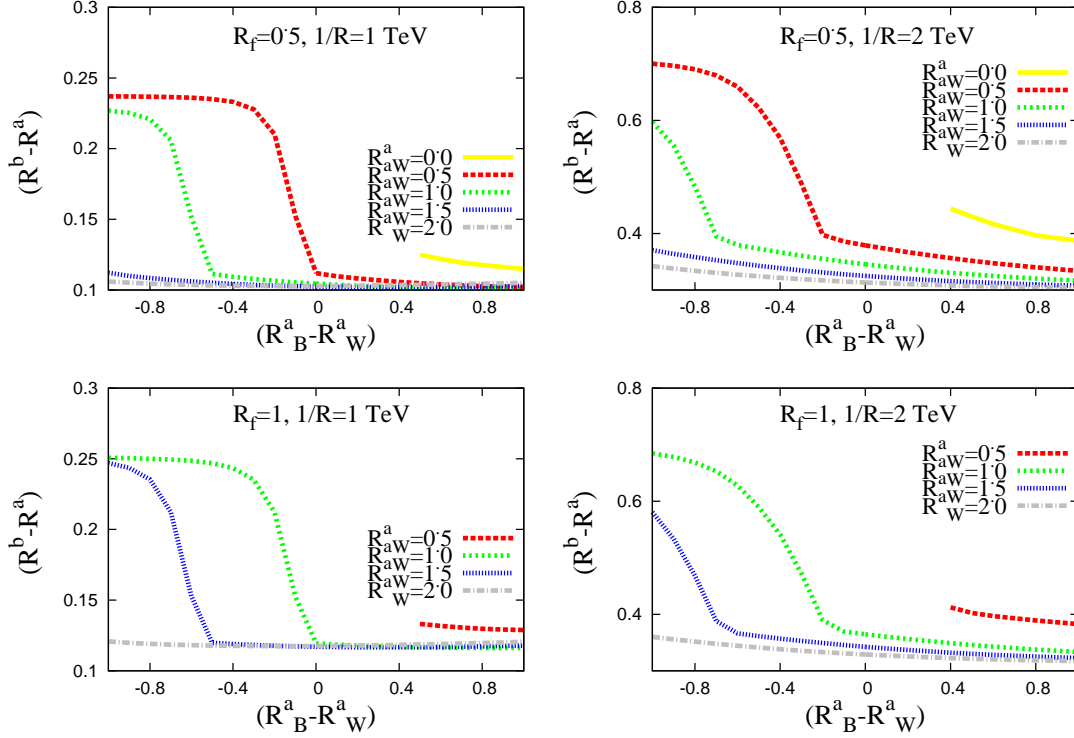


Figure 6: Iso-event curves (40 signal events with  $20 \text{ fb}^{-1}$  data at the LHC running at 8 TeV) for combined  $W_3^1$  and  $B^1$  signals in the  $(R^b - R^a) - (R_B^a - R_W^a)$  plane for several choices of  $R_W^a$  and  $R_f$ . Each panel corresponds to specific values of  $R_f$  and  $R^{-1}$  while each curve in a panel corresponds to a particular value of  $R_W^a$ .  $(R^b - R^a)$  is taken to be the same for  $W_3$  and  $B$ . The regions below the curves correspond to less than 20 events for the chosen  $R_f$  and  $R_W^a$ .  $R^{-1}$  is taken as 1 TeV for the left panels and 2 TeV for the right panels. Note difference in the ordinate scales in the left and right panels.

plane<sup>13</sup> for different choices of  $R_W^a$ ,  $R_f$  and  $R^{-1}$ . The region above the curves will be excluded if the signal is not seen at the projected level. We have checked that the nature of the results is not sensitive to  $R_h$  and we have kept it fixed at -1.1 throughout. In this manner we evade the possibility of the Higgs excitation being the LKP.

At the very outset, we point out that for similar values of input parameters, the 2-lepton rate from  $W_3^1$  production and decay is smaller than that from  $B^1$  approximately by a factor of 4.

We now illustrate a feature of the curves in fig. 6 taking as reference the top left panel ( $R_f = 0.5$ ,  $R^{-1} = 1 \text{ TeV}$ ). The curve for  $R_W^a = 0$  has a different nature from the other curves. For large values of  $(R_B^a - R_W^a)$ , where it exists at all, the curve is away from the other ones which essentially overlap in this region and also, unlike the other curves, it terminates sharply at a value of  $(R_B^a - R_W^a) \simeq 0.5$ . This behaviour can be understood with reference to the  $n = 1$  KK

<sup>13</sup>We have set  $(R^b - R^a)$  to be the same for  $B$  and  $W_3$  while presenting the results in this section just to reduce the number of parameters.

state masses as shown in fig. 1. For  $(R_B^a - R_W^a) \leq 0.5$ , beyond where the curve terminates, the fermion  $n = 1$  state ( $R_f = 0.5$ ,  $R_W^a = 0$ ) becomes the LKP and so this region is excluded. At larger values the  $B^1$  state is the LKP and is admissible. The other point is that with  $R_W^a = 0$  and for the small range of  $(R^b - R^a)$  allowed, the  $n = 1$  fermion states are lighter than  $W_3^1$  which is unlike the rest of the curves of the panel. So, for these latter curves when  $R_B^a$  becomes less than 0.5 the  $B^1$  ( $W_3^1$ ) dominantly decays through KK-conserving (-violating) channels, resulting in the jump in the curves.

Increasing  $(R^b - R^a)$  pushes the  $B^1$  and  $W_3^1$  production cross sections monotonically upwards, hence allowing us to probe higher and higher  $R^{-1}$ . Dependence on  $R^{-1}$  creeps into the cross section via the mass of the KK-gauge bosons. As noted, this extra-dimensional contribution dominates over the part due to gauge symmetry breaking. A higher  $R^{-1}$  implies an enhanced  $m_{G^1}$  which in turn decreases the cross section. This explains the larger  $(R^b - R^a)$  needed to have the same signal rate when we go from the left panels ( $R^{-1} = 1$  TeV) to the right panels ( $R^{-1} = 2$  TeV) of fig. 6. Thus,  $(R^b - R^a)$  and  $R^{-1}$  affect the  $G^1$  production cross section in opposite directions. Increasing the fermion BLKT,  $R_f$ , would result in diminishing the coupling between the SM fermions with the KK-EW-gauge boson (see fig. 3). Thus higher  $(R^b - R^a)$  is necessary to compensate the loss in production rate. This feature is clearly reflected in the difference between the plots in the top and bottom rows of fig. 6.

Let us finally focus on the dependence on  $R_W^a$ . As already pointed out (see fig. 1), larger values of gauge BLKT results in lower KK-gauge boson masses, thus pushing the production rate upward. This explains the lower values of  $(R^b - R^a)$  – hence smaller value of KK-gauge-SM fermion couplings – required to maintain the same production rate in fig. 6 when one compares the different curves in any one panel.

Data have been collected at LHC at 8 TeV proton-proton c.m. energy. Observation or otherwise of the proposed dilepton signal would help in exploring or excluding the parameter space of such non-minimal UED models. The projected exclusion limits can be directly read off from the plots in fig. 6. Any point above a particular iso-event curve can be excluded from the non-observation of such events. In the two fixed point set up, the cross section has a mild dependence on  $R_f$  and  $(R_B^a - R_W^a)$ . The  $r_f$  dependence of the cross section comes only through the coupling. A careful examination of the coupling in eqs. (33) and (36) shows that it tends to a constant as  $R_f \rightarrow \infty$ .

## V.2 Fermion and gauge boson BLKT at one fixed point only

Now let us turn to the case of BLKTs at only one fixed point (fig. 7). The relevant KK-parity violating couplings vanish when<sup>14</sup>  $R_f = R_G$  where  $G \equiv W$  or  $B$  as noted from eq. (36). This is seen in fig. 4 for different choices of  $R_f$ . So, the production mode we consider here is not available. Further, in this situation, the  $n = 1$  gauge boson and fermion states are mass degenerate and KK-number conserving decay modes are also not allowed. In the neighbourhood of this point there is an important asymmetry, however, between whether  $R_{B,W}$  is more than

---

<sup>14</sup>Since for this option the BLKTs are present at only one fixed point we denote them by  $R_f$ ,  $R_W$ , and  $R_B$ .

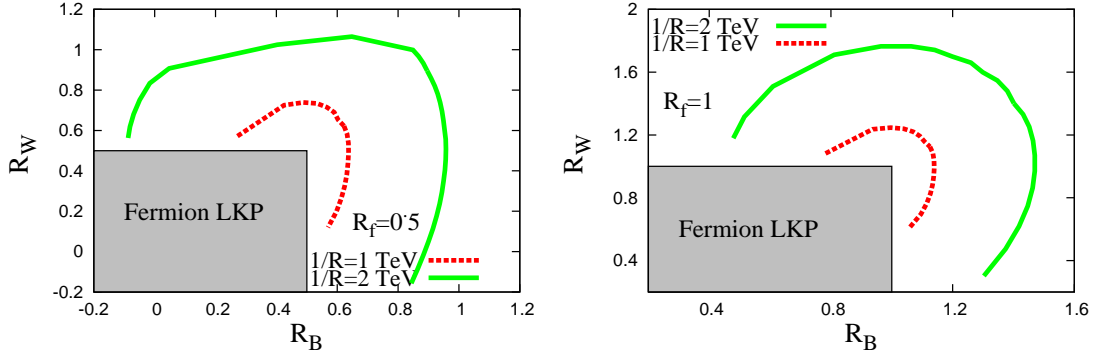


Figure 7: Iso-event curves (40 signal events with  $20 \text{ fb}^{-1}$  data at the LHC running at 8 TeV) for combined  $W_3^1$  and  $B^1$  signals in the  $R_W - R_B$  plane when the BLKTs are present at only one of the two fixed points. The region enclosed by the solid green (dashed red) curve and the fermion LKP box yields less than 20 events for  $R^{-1} = 2 \text{ TeV}$  (1 TeV). The left (right) panel corresponds to  $R_f = 0.5$  (1.0). Note difference in scales in the two panels.

$R_f$  or less. In the former case, the gauge boson  $n = 1$  state is lighter than the corresponding fermion state and KK-number conserving decays are not kinematically possible. As shown in fig. 5 the KK-number violating decay branching ratio is high. In the latter case, the KK-number conserving decay is allowed for the  $n = 1$  gauge boson and so the desired branching ratio to zero-mode fermions is small. Of course, if both  $R_B$  and  $R_W$  are smaller than  $R_f$  then the fermion state is the LKP.

The evidence of the above observations can be readily found in the two panels of fig. 7. For any of the iso-event contours, the largest value of  $R_B$  will be for  $R_W = R_f$  and *vice-versa*. This is because when  $R_W = R_f$  there is no contribution to the signal from the  $W_3^1$  as discussed above. As  $R_W$  shifts from this value the contribution from  $W_3^1$  reduces the needed  $R_B$ . But this is not symmetric because of the difference in the branching ratios of  $W_3^1$  on the two sides of  $R_f$  as is seen from Fig. 5.

We have presented the iso-event curves (again 40 events with  $20 \text{ fb}^{-1}$  luminosity) for this scenario in the  $R_W^a - R_B^a$  plane. We also show the excluded region where the  $n = 1$  fermion is the LKP. In accordance with the preceding discussion, it is readily seen that for the point  $R_W = R_B = R_f$  the KK-number violating coupling is zero and also the  $n = 1$  states are all degenerate. So, neither KK-number violating nor conserving decays are permitted.

## VI Conclusions

To summarize, we have considered the effects of boundary localized kinetic terms in a situation where all the SM fields can propagate in a spacetime with four spatial and one timelike dimensions. The extra spatial dimension  $y$  is compact and can be considered as a circle of radius

$R$  and also has a  $y \leftrightarrow -y$  symmetry. Consequently there are two fixed points at  $y = 0$  and  $y = \pi R$ . At these boundary points one can include terms consistent with 4-dimensional Lorentz symmetry. These are either kinetic terms or mass terms. We concentrate on the former.

In the minimal Universal Extra Dimensional model, radiative corrections play a crucial role in removing the near-degeneracy of the masses of the KK-modes of all SM particles of the same level,  $n$ . UED, being an effective theory, is defined with a cut-off,  $\Lambda$ . In mUED the boundary terms are chosen in a manner such that at  $\Lambda$  the contribution due to radiative corrections vanishes. In this process, instead of calculating the radiative correction in a 5d set up one can also parametrise these effects by incorporating a set of BLKTs.

There are two possibilities of choosing the BLKTs with rather distinct physics consequences. In the first, the BLKTs are of equal strength at both the boundary points ( $y = 0, \pi R$ ). Here, a  $Z_2$  symmetry  $y \longleftrightarrow (y - \pi R)$  remains. One then ends up with a theory where the spectrum of KK-particles and the couplings can be drastically different from mUED. The lightest among the  $n = 1$  KK particles can be a dark matter candidate. The other alternative is to allow the BLKTs at  $y = 0$  and  $y = \pi R$  to be of unequal strengths. This will lead to a breakdown of KK-parity and will allow, for example, the decay we have examined,  $B^1(W_3^1) \rightarrow e^+e^-, \mu^+\mu^-$ , and production of the  $B^1(W_3^1)$  singly.

In this article, we have considered the possible BLKTs for an interacting theory of *only* fermions and the neutral electroweak gauge bosons. In one alternative, the strengths of fermion BLKTs at the two fixed points have been assumed to be equal  $\equiv r_f$ . For the gauge boson boundary kinetic terms we have considered the general case of unequal BLKTs ( $r_G^a \neq r_G^b$ ). Equality of the latter strengths would restore a  $Z_2$ -parity. As an alternate possibility we have considered the situation where the fermion and gauge boson BLKTs are present *only* at the  $y = 0$  fixed point. Presence of the boundary terms modify the field equations in the  $y$ -direction. Consistency conditions of the solutions of the above equations lead to the masses of KK-excitations of fermions and the photon.

For the purpose of illustration, we have calculated the coupling of  $W_3^1$  and  $B^1$ , the  $n = 1$  KK-excitations of the neutral electroweak gauge bosons, to a pair of zero-mode fermions (i.e., SM fermions) as a function of  $r_f, r^a, r^b$  and  $R^{-1}$ . In general, we have presented the couplings as a function of the scaled variable  $(R^b - R^a)$  for several choices of the other parameters. This coupling is a hallmark of KK-parity violation and vanishes in the  $(R^b - R^a) = 0$  limit. A similar KK-parity violating coupling, which arises when the BLKTs are present only at  $y = 0$ , has also been evaluated. Finally, the production and decay of  $W_3^1$  and  $B^1$  at the LHC, via the above KK-parity violating coupling, have been considered. We have investigated the viability of the *dilepton* signature at the LHC running at 8 TeV  $pp$  center of mass energy. It is revealed that non-observation of such a high mass *dilepton* signal with  $20 \text{ fb}^{-1}$  accumulated luminosity in the 8 TeV run of LHC will disfavour a large part of the parameter space (spanned by  $r_f, r^a, r^b$  and  $R^{-1}$ ).

This particular new physics signal can also arise if there are extra  $Z$ -like bosons in the context of extensions of the SM, e.g., the Left-Right symmetric models or models with an extra  $U(1)$  symmetry. We have not attempted to compare the signals of the model under consideration

with those in these other scenarios.

Let us briefly comment here on the numerical values of some of the input parameters. In ref. [21] constraints on the BLKT parameters have been derived from the consideration of electroweak precision variables  $S$ ,  $T$ , and  $U$ . In this work the authors have considered a particular choice of gauge BLKT parameters, namely, they have set  $R_W^a = R_B^a$ . As pointed out in an earlier section, this choice of BLKT would lead to the same mixing at all levels  $n$  as for the zero modes, i.e., the weak mixing angle ( $28^\circ$ ) in each KK-level. On the other hand, in general,  $\theta_W^n$  is negligibly small for unequal  $U(1)$  and  $SU(2)$  BLKTs. It is well known that the value of  $\theta_W$  plays a crucial role in the exercise done with precision observables and so the constraints derived in [21] are not directly applicable here.

Our analysis is simple-minded in the sense that we have not considered the effects of initial and final state radiations, showering and detector effects while estimating the signal cross section. Our demarcations of the excluded regions should therefore be considered only as indicative.

**Acknowledgements** AD acknowledges partial support from the DRS project sanctioned to the Department of Physics, University of Calcutta by the University Grants Commission. UKD is supported by funding from the Department of Atomic Energy, Government of India for the Regional Centre for Accelerator-based Particle Physics, Harish-Chandra Research Institute (HRI). AS is the recipient of a Junior Research Fellowship from the University Grants Commission. AR is thankful to the Department of Science and Technology for a J.C. Bose Fellowship.

## References

- [1] T. Appelquist, H. C. Cheng and B. A. Dobrescu, Phys. Rev. D **64** (2001) 035002 [arXiv:hep-ph/0012100].
- [2] H. Georgi, A. K. Grant and G. Hailu, Phys. Lett. B **506** (2001) 207 [arXiv:hep-ph/0012379].
- [3] H.C. Cheng, K.T. Matchev and M. Schmaltz, Phys. Rev. D **66** (2002) 036005 [arXiv:hep-ph/0204342].
- [4] H. C. Cheng, K. T. Matchev and M. Schmaltz, Phys. Rev. D **66** (2002) 056006 [arXiv:hep-ph/0205314].
- [5] C. Csaki, C. Grojean, L. Pilo and J. Terning, Phys. Rev. Lett. **92** (2004) 101802 [arXiv:hep-ph/0308038]; C. Csaki, C. Grojean, J. Hubisz, Y. Shirman and J. Terning, Phys. Rev. D **70** (2004) 015012 [arXiv:hep-ph/0310355].
- [6] P. Dey and G. Bhattacharyya, Phys. Rev. D **70** (2004) 116012 [arXiv:hep-ph/0407314]; P. Dey and G. Bhattacharyya, Phys. Rev. D **69** (2004) 076009 [arXiv:hep-ph/0309110].
- [7] P. Nath and M. Yamaguchi, Phys. Rev. D **60** (1999) 116006 [arXiv:hep-ph/9903298].

- [8] D. Chakraverty, K. Huitu and A. Kundu, Phys. Lett. B **558** (2003) 173 [arXiv:hep-ph/0212047].
- [9] A.J. Buras, M. Spranger and A. Weiler, Nucl. Phys. B **660** (2003) 225 [arXiv:hep-ph/0212143]; A.J. Buras, A. Poschenrieder, M. Spranger and A. Weiler, Nucl. Phys. B **678** (2004) 455 [arXiv:hep-ph/0306158].
- [10] K. Agashe, N.G. Deshpande and G.H. Wu, Phys. Lett. B **514** (2001) 309 [arXiv:hep-ph/0105084]; U. Haisch and A. Weiler, Phys. Rev. D **76** (2007) 034014 [hep-ph/0703064 [HEP-PH]].
- [11] J. F. Oliver, J. Papavassiliou and A. Santamaria, Phys. Rev. D **67** (2003) 056002 [arXiv:hep-ph/0212391].
- [12] T. Appelquist and H. U. Yee, Phys. Rev. D **67** (2003) 055002 [arXiv:hep-ph/0211023]; G. Belanger, A. Belyaev, M. Brown, M. Kakizaki and A. Pukhov, EPJ Web Conf. **28** (2012) 12070 [arXiv:1201.5582 [hep-ph]].
- [13] T.G. Rizzo and J.D. Wells, Phys. Rev. D **61** (2000) 016007 [arXiv:hep-ph/9906234]; A. Strumia, Phys. Lett. B **466** (1999) 107 [arXiv:hep-ph/9906266]; C.D. Carone, Phys. Rev. D **61** (2000) 015008 [arXiv:hep-ph/9907362].
- [14] I. Gogoladze and C. Macesanu, Phys. Rev. D **74** (2006) 093012 [arXiv:hep-ph/0605207].
- [15] T. Rizzo, Phys. Rev. D **64** (2001) 095010 [arXiv:hep-ph/0106336]; C. Macesanu, C.D. McMullen and S. Nandi, Phys. Rev. D **66** (2002) 015009 [arXiv:hep-ph/0201300]; Phys. Lett. B **546** (2002) 253 [arXiv:hep-ph/0207269]; H.-C. Cheng, Int. J. Mod. Phys. A **18** (2003) 2779 [arXiv:hep-ph/0206035]; A. Muck, A. Pilaftsis and R. Rückl, Nucl. Phys. B **687** (2004) 55 [arXiv:hep-ph/0312186]; B. Bhattacharjee and A. Kundu, J. Phys. G **32** (2006) 2123 [arXiv:hep-ph/0605118]; B. Bhattacharjee and A. Kundu, Phys. Lett. B **653** (2007) 300 [arXiv:0704.3340 [hep-ph]]; G. Bhattacharyya, A. Datta, S. K. Majee and A. Raychaudhuri, Nucl. Phys. B **821** (2009) 48 [arXiv:hep-ph/0608208]; P. Bandyopadhyay, B. Bhattacharjee and A. Datta, JHEP **1003** (2010) 048 [arXiv:0909.3108 [hep-ph]]; B. Bhattacharjee, A. Kundu, S. K. Rai and S. Raychaudhuri, Phys. Rev. D **81** (2010) 035021 [arXiv:0910.4082 [hep-ph]]; D. Choudhury, A. Datta and K. Ghosh, JHEP **1008** (2010) 051 [arXiv:0911.4064 [hep-ph]]; B. Bhattacharjee and K. Ghosh, Phys. Rev. D **83** (2011) 034003 [arXiv:1006.3043 [hep-ph]]; H. Murayama, M. M. Nojiri and K. Tobioka, Phys. Rev. D **84** (2011) 094015 [arXiv:1107.3369 [hep-ph]]; K. Nishiwaki, K. -y. Oda, N. Okuda and R. Watanabe, Phys. Lett. B **707** (2012) 506 [arXiv:1108.1764 [hep-ph]]; [arXiv:1111.2912 [hep-ph]].
- [16] G. Bhattacharyya, P. Dey, A. Kundu and A. Raychaudhuri, Phys. Lett. B **628** (2005) 141 [arXiv:hep-ph/0502031]; B. Bhattacharjee and A. Kundu, Phys. Lett. B **627** (2005) 137 [arXiv:hep-ph/0508170]; A. Datta and S. K. Rai, Int. J. Mod. Phys. A **23** (2008) 519 [arXiv:hep-ph/0509277]; B. Bhattacharjee, A. Kundu, S. K. Rai and S. Raychaudhuri, Phys. Rev. D **78** (2008) 115005 [arXiv:0805.3619 [hep-ph]]; B. Bhattacharjee, Phys. Rev. D **79** (2009) 016006 [arXiv:0810.4441 [hep-ph]].

- [17] C. Schwinn, Phys. Rev. D **69** (2004) 116005 [arXiv:hep-ph/0402118].
- [18] G. R. Dvali, G. Gabadadze, M. Kolanovic and F. Nitti, Phys. Rev. D **64** (2001) 084004 [arXiv:hep-ph/0102216].
- [19] M. S. Carena, T. M. P. Tait and C. E. M. Wagner, Acta Phys. Polon. B **33** (2002) 2355 [arXiv:hep-ph/0207056].
- [20] F. del Aguila, M. Perez-Victoria and J. Santiago, JHEP **0302** (2003) 051 [hep-th/0302023]; hep-ph/0305119.
- [21] F. del Aguila, M. Perez-Victoria and J. Santiago, Acta Phys. Polon. B **34** (2003) 5511 [hep-ph/0310353].
- [22] T. Flacke, A. Menon and D. J. Phalen, Phys. Rev. D **79** (2009) 056009 [arXiv:0811.1598 [hep-ph]].
- [23] For a discussion of BLKT in extra-dimensional QCD, see A. Datta, K. Nishiwaki and S. Niyogi, arXiv:1206.3987 [hep-ph], JHEP (to appear).
- [24] J. Pumplin *et al.*, JHEP **07** (2002) 012.